DOI: 10.31319/2519-8106.2(53)2025.341962

UDC 621.313.323

**Kachura Oleksii**, candidate of technical sciences, associate professor at the Department of Electronics and Electronic Communications

**Качура О.В.**, кандидат технічних наук, доцент кафедри електроніки та електронних комунікацій

ORCID: 0000-0002-6338-0974

e-mail: fem@ukr.net

**Gulesha Olena**, candidate of pedagogical sciences, associate professor at the Department of Electronics and Electronic Communications

**Гулєша О.М.**, кандидат педагогічних наук, доцент кафедри електроніки та електронних комунікацій

ORCID: 0000-0002-7512-5671 e-mail: e.gulesha@gmail.com

**Trikilo Alik**, candidate of technical sciences, associate professor at the Department of Electronics and Electronic Communications

**Трикіло А.І.**, кандидат технічних наук, доцент кафедри електроніки та електронних комунікацій

ORCID: 0000-0002-5203-5948

e-mail: 3kilo@i.ua

**Kolychev Serhiy**, candidate of technical sciences, associate professor at the Department of Electrical Engineering and Electromechanics

**Количев С.В.**, кандидат технічних наук, доцент кафедри електротехніки та електромеханіки ORCID: 0000-0002-1017-5125

e-mail: kolychev.sergey58@gmail.com

**Roenko Yukhym**, Senior Lecturer, Department of Electrical Engineering and Electromechanics **Роєнко Ю.С.**, старший викладач кафедри електротехніки та електромеханіки

Роснко Ю.С., старший викладач кафедри електротехніки та електромеханіки

ORCID: 0000-0001-9408-2171 e-mail: efim.mail@gmail.com

Dniprovsky State Technical University, Kamianske Дніпровський державний технічний університет, м. Кам'янське

# MODEL OF AN INDUCTION MOTOR WITH A SOLID FERROMAGNETIC ROTOR FOR DYNAMIC MODES

# МОДЕЛЬ АСИНХРОННОГО ДВИГУНА З МАСИВНИМ ФЕРОМАГНІТНИМ РОТОРОМ ДЛЯ ДИНАМИЧНИХ РЕЖИМІВ

The introduction of automated lines in various areas of industrial production requires an assessment of the quality and operating conditions of electric drives. This leads to an expansion of the requirements for electric motors, which must maintain operability under different conditions. Today, induction motors are widely used for industrial mechanism drives. A special place among them is occupied by induction motors with a solid rotor (IMSR), which have the following advantages over general industrial ones: high mechanical strength, operation at high rotation speeds, ease and technological capability of manufacture, long service life, high overloading. Given the advantages of IMSR, it is relevant to study their characteristics for various design modifications in order to expand the scope of industrial application. Taking into account the design diversity of IMSR, the use of analytical methods

for calculating their characteristics is difficult. The solution is the use of numerical methods, among which the most widely used is the finite element method (FEM). The article proposes a universal mathematical model of an induction motor with a solid rotor based on the finite element method, which allows studying electromagnetic and electromechanical processes in dynamic modes.

**Keywords**: induction motor with a solid rotor, finite element method, dynamic mode, system of equations.

Впровадження у різних сферах промислового виробництва автоматизованих технологічних ліній вимагає оцінки якості та умов експлуатації електроприводів виконавчих механізмів. Це обумовлює розширення вимог до електродвигунів, які повинні зберігати функціональність у широких діапазонах температур, високій вологості, в умовах вібрацій і ударів, коливань напруги живлення і т.д. Дані фактори суттєво впливають на робочі властивості електродвигунів, а тому повинні враховуватися при їх проектуванні.

На сьогоднішній день асинхронні двигуни (АД) набули широкого поширення для промислових механізмів. Особливе місце серед них займають асинхронні двигуни з твердотілим ротором (АДТР), які у порівнянні із загальнопромисловими серіями АД мають наступні переваги: висока механічна міцність, робота на великих частотах обертання, простота та технологічність виготовлення, тривалий термін служби, висока перевантажувальна здатність, прийнятні пускові та робочі характеристики. Враховуючи переваги АДТР, актуальним є дослідження їх характеристик для різних конструктивних модифікацій з метою розширення сфер промислового застосування.

Асинхронні двигуни з твердотілим ротором мають конструктивні особливості і відрізняються від загальнопромислових асинхронних двигунів насамперед формою ротора, який, як правило, виготовляється із магнітної сталі. Це впливає не тільки на характеристики двигуна, але і на динаміку перехідних процесів, що залежить від інерції як самого АДТР, так і ланок виконавчого механізму.

Зважаючи на конструктивне різноманіття АДТР, використання аналітичних методів для розрахунку їх характеристик є проблематичним. Виходом є застосування чисельних методів, серед яких найбільшого поширення набув метод кінцевих елементів. У статті запропоновано універсальну математичну модель асинхронного двигуна з твердотілим ротором на основі методу кінцевих елементів, яка дозволяє досліджувати електромагнітні та електромеханічні процеси у динамічних режимах.

**Ключові слова**: асинхронний двигун з твердотілим ротором, метод кінцевих елементів, динамічний режим, система рівнянь.

## **Problem's Formulation**

A significant part of the generated electric power is converted into mechanical power by electric machines, the largest part of which is made up of induction motors (IM). In modern conditions, increasingly high requirements are imposed on IM: compactness, manufacturability, reliability, high energy indicators. To meet these requirements, it is necessary to create new designs of electric motors with special properties and parameters. One of the promising direction in this area is the induction motor with a massive rotor. The advantages of this design include: 1) high mechanical strength, allowing high rotation speeds; 2) simplicity and technological capability of manufacture; 3) long service life; 4) high overload capacity; 5) acceptable starting properties.

## Analysis of recent research and publications

A number of works are devoted to the study of IMSR [1—4]. Thus, in [1] a review of motors with a massive rotor is presented, covering the areas of their use, the features of the operation of electric motors in difficult conditions and safety-critical installations are considered. The paper presents a classification of IMSR based on various rotor topologies, emphasizing unique design features and performance characteristics. Particular attention is paid to the issues of multiphysical modeling of IMSR, including electromagnetic, mechanical and thermal processes. The paper proposes a multi-stage method for calculating the characteristics of motors, graphs of current density in the rotor and their harmonic composition for various frequencies are obtained.

The paper [2] considers the process of designing an asynchronous motor with a solid rotor

with a power of 18 MW and a rotor speed of 12,000 rpm. The authors propose an original rotor design with axial slots and copper end rings. The paper develops a mathematical model of the motor based on the finite element method with step-by-step time control. As a result of modeling electromagnetic processes, magnetic flux density distribution patterns in the motor cross-section and in the air gap were obtained both in the idle mode and when the shaft is subjected to a load torque. Based on the obtained electromagnetic parameters, instantaneous current values in the stator windings, electromagnetic torque values, and currents flowing in the end short-circuiting copper rings were calculated. In addition, the paper analyzes steel losses caused by the main and harmonic fields. The authors conclude that the designed motor has acceptable characteristics and good performance.

In [3], a new solid rotor topology for electric machines with internal permanent magnets is proposed, which is used in the design of starter-generators for the aviation industry. It is shown that the key problem in the design of such electric motors is to meet the conditions of high torque at startup and high speed in the nominal operating mode. The authors propose to manufacture such rotors from semi-magnetic stainless steel, which has a higher yield strength compared to laminated steel. To maintain the required stress levels, a new slotted rotor design was developed, which was tested using electromagnetic, static structural and dynamic structural finite element analysis. To confirm the proposed concepts, a series of experiments were conducted, based on which it was shown that the proposed rotor design meets the mechanical, thermal and magnetic requirements.

In the work [4] a high-speed 15 kW IM with a slot rotor and a nominal rotation speed of 120 thousand rpm is considered. Based on analytical dependencies, the volumetric size of the IMSR is determined, its two-dimensional finite element model is constructed, which made it possible to establish the influence of the number and shape of the rotor slots on the motor torque. The work established that the matching scheme of the slots of a solid rotor has a significant effect on the torque pulsation, and the slot size on the electromagnetic and mechanical properties.

Despite the fact that IMSRs have a relatively simple mechanical parts, issues related to their design often cause difficulties. Existing analytical methods for designing IMSRs are usually oriented toward a specific rotor design and, with minimal modifications, do not ensure the correctness of the results obtained. In addition, strong saturation of the tooth zone, distortion of magnetic induction in the air gap due to the presence of high harmonics, significant temperature loads, and intermittent short-term operating modes are far from a complete list of factors that have a negative impact on the accuracy of the calculation.

In this regard, numerical methods are becoming an important tool for analyzing IMSR, among which the finite element method can be singled out [5—9]. The advantages of FEM compared to classical design methods include the ability to study the parameters of the electromagnetic field in electromechanical objects of arbitrary design, taking into account the nonlinear properties of materials in both stationary and dynamic modes. In addition, by combining the FEM equations with the equations of electrical circuits, models can be implemented for calculating the electromechanical characteristics of IMSR, taking into account the features of the supply circuits. To create a mathematical model of IMSR, we will use FEM.

#### Formulation of the study purpose

Develop a universal mathematical model of the IMSR, which allows to study electromagnetic and electromechanical processes in dynamic operating modes, taking into account the nonlinear properties of the materials used and the design features of the engine.

To achieve the stated goal, the following tasks were solved in the paper:

- a numerical mathematical model of the IMSR was created based on the FEM;
- electric circuit equations for the IMSR winding phases were written based on Kirchhoff's laws;
- a combined mathematical model was created based on the unification of the numerical model of the IMSR and the equations of electric circuits, which allows to analyze electromagnetic and electromechanical processes over time;
- the adequacy of the created model was checked by calculating the transient processes of starting and loading the IMSR based on the serial IM UAD-32 with a modified rotor.

### **Presenting main material**

To calculate the IMSR's parameters, we use the Maxwell equations system, which in the SI system takes the form [13]:

$$rot \vec{H} = \vec{J};$$

$$rot \vec{E} = -\partial \vec{B}/\partial t;$$

$$div \vec{D} = \rho;$$

$$div \vec{B} = 0,$$
(1)

where  $\vec{H}$  — the intensity of the magnetic field;  $\vec{J}$  — density of electric current;  $\vec{E}$  — electric field strength;  $\vec{B}$  — magnetic induction;  $\rho$  is the density of electric charge.

Equations characterizing the electromagnetic properties of the material environment are added to the equations (1):

$$\vec{D} = \varepsilon \vec{E};$$

$$\vec{B} = \mu \vec{H};$$

$$\vec{J} = \sigma \vec{E}.$$
(2)

where  $\varepsilon$  — dielectric permeability;  $\mu$  — magnetic permeability;  $\sigma$  — specific conductivity of the environment.

As a rule, the system (1) is not solved in its initial form. It is usually transformed into another in which vectors  $\vec{E}$ ,  $\vec{B}$  and  $\vec{H}$  are replaced by auxiliary functions. In particular, introducing the concept of vector magnetic potential [13], we come to the expression

$$\vec{B} = rot \ \vec{A} \ . \tag{3}$$

Having performed a number of known mathematical transformations [13], we obtain a general equation that describes an electromagnetic field

$$\nabla \times \left(\nu \nabla \times \vec{A}\right) = J - \sigma \frac{\partial \vec{A}}{\partial t}, \tag{4}$$

where  $\nabla$  — the nabla operator;  $\nu$  — specific magnetic resistance of steel.

The equation (4) is generalized, the right part of which depends on the analyzed environment, and in vacuum is transformed into Laplace equation:

$$\nabla \times (\nu \nabla \times \vec{A}) = 0.$$

A solution (4) is related to the solution of the three-dimensional field problem that in the cartesian system of coordinates assumes as

$$\frac{\partial}{\partial x} \left( v \frac{\partial A}{\partial x} \right) + \frac{\partial}{\partial y} \left( v \frac{\partial A}{\partial y} \right) + \frac{\partial}{\partial z} \left( v \frac{\partial A}{\partial z} \right) = J - \sigma \frac{\partial A}{\partial t}, \tag{5}$$

where x, y, z — the coordinates of the region.

In an expanded form (4) in relation to IMSR may be presented as

$$\nabla \times (v\nabla \times \vec{A}) = 0 - air \ gap;$$

$$\nabla \times (v\nabla \times \vec{A}) = 0 - stator;$$

$$\nabla \times (v\nabla \times \vec{A}) = \frac{N_w i_w}{S_w} - the \ stator \ slot;$$

$$\nabla \times (v\nabla \times \vec{A}) = -\sigma \frac{\partial A}{\partial t} - \upsilon \left(\frac{\partial A}{\partial x} - \frac{\partial A}{\partial y}\right) - rotor;$$

$$\nabla \times (v\nabla \times \vec{A}) = -\sigma \frac{\partial A}{\partial t} - \upsilon \left(\frac{\partial A}{\partial x} - \frac{\partial A}{\partial y}\right) - shaft,$$

$$(6)$$

where w — index of the corresponding phase winding; i — current in phase winding;  $N_w$ ,  $S_w$  — the number of turns and the cross-sectional area; v — the speed of the rotor.

Let's simplify the task, going from three-dimensional to two-dimensional. In a rectangular two-dimensional coordinate system (6) transforms to the form:

$$\frac{\partial}{\partial x} \left( v \frac{\partial A}{\partial x} \right) + \frac{\partial}{\partial y} \left( v \frac{\partial A}{\partial y} \right) = 0 - air \ gap;$$

$$\frac{\partial}{\partial x} \left( v \frac{\partial A}{\partial x} \right) + \frac{\partial}{\partial y} \left( v \frac{\partial A}{\partial y} \right) = 0 - stator;$$

$$\frac{\partial}{\partial x} \left( v \frac{\partial A}{\partial x} \right) + \frac{\partial}{\partial y} \left( v \frac{\partial A}{\partial y} \right) = \frac{N_w \times i_x}{S_w} - the \ stator \ slot;$$

$$\frac{\partial}{\partial x} \left( v \frac{\partial A}{\partial x} \right) + \frac{\partial}{\partial y} \left( v \frac{\partial A}{\partial y} \right) = -\sigma \frac{\partial A}{\partial t} - \upsilon \left( \frac{\partial A}{\partial x} - \frac{\partial A}{\partial y} \right) - rotor;$$

$$\frac{\partial}{\partial x} \left( v \frac{\partial A}{\partial x} \right) + \frac{\partial}{\partial y} \left( v \frac{\partial A}{\partial y} \right) = -\sigma \frac{\partial A}{\partial t} - \upsilon \left( \frac{\partial A}{\partial x} - \frac{\partial A}{\partial y} \right) - shaft.$$
(7)

The system (7) must be supplemented by the voltage equation for each phase winding of IMSR

$$\left\{\mathbf{u}_{\mathbf{x}}\right\} = \left[\mathbf{r}_{\mathbf{x}}\right] \left\{\mathbf{i}_{\mathbf{x}}\right\} + \frac{N_{w}l}{S_{w}} \left\{ \int_{S_{w}} \frac{\partial A}{\partial t} dS_{w} \right\} + L_{l} \frac{d\left\{\mathbf{i}_{\mathbf{x}}\right\}}{dt}$$
(8)

and the main equation of rotating motion dynamics

$$M - M_c = J \frac{d\omega}{dt}, \tag{9}$$

where  $\{\mathbf{u_x}\}$  — the vector of phase voltages applied to the winding;  $[\mathbf{r_x}]$  — matrix of ohmic resistances of IMSR phase winding;  $\{\mathbf{i_x}\}$  — current vector in phase windings;  $L_l$  — inductivity of the frontal parts; l — conductor length; M — the magnitude of the electromagnetic moment;  $M_c$  — static moment of resistance on the shaft; J — the moment of inertia of the rotor;  $\omega$  — the angular speed of rotation of the rotor.

The task of the solution (7) is to solve Poisson equations regarding vector magnetic potential. Given the complexity of IMSR's geometry, the use of analytical methods for its solution is problematic. The way out is the transformation of the border problem into variational and use of FEM [11, 12].

The variational formulation of the problem involves the use of energy functional [5] and its minimization

$$F(A) = \int_{S} \left( \int_{0}^{Bx} \frac{Bx}{\mu \mu_0} dBx + \int_{0}^{By} \frac{By}{\mu \mu_0} dBy \right) - \int_{S} AjdS, \qquad (10)$$

where S is the area of the finite element;  $B_x, B_y$  — components of magnetic induction vector; j — current density vector in the finite element.

Based on the variational formulation for (7), we obtain a system of differential equations of the first order in the matrix form [5]:

$$[\mathbf{S}] \{\mathbf{A}\} + [\mathbf{N}] \frac{\partial \{\mathbf{A}\}}{\partial t} = \{\mathbf{F}\}. \tag{11}$$

The corresponding matrices look like:

$$[\mathbf{S}] = \sum_{e=1}^{N_e} \left( \frac{v}{4\Delta^e} [\mathbf{K}]^e \right);$$

$$\left\{ \mathbf{F} \right\} = \sum_{e=1}^{N_e} \frac{w}{\Omega_o} \frac{\Delta^e}{3} \cdot i \; ;$$

$$[\mathbf{N}] = \sum_{e=1}^{N_e} \frac{\sigma \,\Delta}{12} [\mathbf{Q}],$$

where e is an element of the finite area;  $N_e$  — the number of elements to which the calculated area is discretized;  $\Delta^e$  — element area; i — current in the winding of the phase;  $\Omega$  — the cross-sectional area of the coil;  $[\mathbf{K}]$  — global hardness matrix;  $[\mathbf{Q}]$  — dumpling matrix [5].

The area of the finite element is calculated as

$$\Delta^{e} = x_{j} y_{k} - y_{j} x_{k} + x_{i} y_{j} - x_{i} y_{k} + y_{i} x_{k} - y_{i} x_{j},$$

where i, j, k — element indexes.

Matrices [K] and [Q] look like:

$$[\mathbf{K}]^{e} = \begin{bmatrix} \left(b_{i}^{e}\right)^{2} + \left(g_{i}^{e}\right)^{2} & b_{i}^{e}b_{j}^{e} + g_{i}^{e}g_{j}^{e} & b_{i}^{e}b_{k}^{e} + g_{i}^{e}g_{k}^{e} \\ b_{i}^{e}b_{j}^{e} + g_{i}^{e}g_{j}^{e} & \left(b_{j}^{e}\right)^{2} + \left(g_{j}^{e}\right)^{2} & b_{j}^{e}b_{k}^{e} + g_{j}^{e}g_{k}^{e} \\ b_{i}^{e}b_{k}^{e} + g_{i}^{e}g_{k}^{e} & b_{j}^{e}b_{k}^{e} + g_{j}^{e}g_{k}^{e} & \left(b_{k}^{e}\right)^{2} + \left(g_{k}^{e}\right)^{2} \end{bmatrix};$$

$$[\mathbf{Q}]^{e} = \begin{bmatrix} 2 & 1 & 1 \\ 1 & 2 & 1 \\ 1 & 1 & 2 \end{bmatrix}.$$

The coefficients of the matrix  $[\mathbf{K}]^e$  will be found by formulas:

$$\beta_i^e = y_j - y_k; \ \beta_j^e = y_k - y_i; \ \beta_k^e = y_i - y_j;$$
  
$$\gamma_i^e = x_k - x_j; \ \gamma_j^e = x_i - x_k; \ \gamma_k^e = x_j - x_i.$$

In the case of stationary processes (11) will turn into a look:

$$[K]{A} = {F}.$$

Determining the value of magnetic induction and intensity at each point of the field of the IMSR area, we find electromagnetic force and rotating moment through tensions [11]. If the tension system  $\overline{T}_n$  on the surface S is equivalent to electromagnetic force acting on some volume V, then this force can be found by adding elementary tension forces  $\overline{T}_n dS$ :

$$\overline{F} = \iint_{S} \overline{T}_{n} dS = \overline{q}_{x} F_{x} + \overline{q}_{y} F_{y} + \overline{q}_{z} F_{z} ,$$

where

$$F_x = \iint_S T_{nx} dS$$
 ,  $F_y = \iint_S T_{ny} dS$  ,  $F_z = \iint_S T_{nz} dS$  .

The electromagnetic torque acting on the allocated volume will be found by adding its components relative to the axes x, y, z:

$$\overline{M} = \iint_{S} \left[ \overline{\mathbf{r}} \, \overline{\mathbf{T}}_{\mathbf{n}} \right] dS = \overline{q}_{x} M_{x} + \overline{q}_{y} M_{y} + \overline{q}_{z} M_{z} ,$$

where

$$\begin{split} \boldsymbol{M}_{x} &= \overline{q}_{x} \overline{\boldsymbol{M}} = \iint_{S} \left( y T_{nz} - z T_{ny} \right) dS \ ; \\ \boldsymbol{M}_{y} &= \overline{q}_{y} \overline{\boldsymbol{M}} = \iint_{S} \left( z T_{nx} - x T_{nz} \right) dS \ ; \end{split}$$

$$M_z = \overline{q}_z \overline{M} = \iint_S (xT_{ny} - yT_{nx}) dS$$
.

The values  $T_{nx}$ ,  $T_{ny}$ ,  $T_{nz}$  — components of the tensor along the axes of the coordinate system.

The tensor of tension through the parameters of the field in vector form is defined as [13]

$$\overline{T}_n = \frac{\overline{B}B_n - 0.5B^2\overline{n}}{\mu\mu_0},$$

where  $\overline{B}$  — the induction vector at the field point;  $B_n$  — normal component of induction;  $\overline{n}$  — normal orth to the side of the surface on which the tension operates  $\overline{T}_n$ .

Tensor tension components look like [13]:

$$\begin{split} T_{xx} &= \frac{B_x^2 - 0.5B^2}{\mu\mu_0} \; ; \; T_{xy} = \frac{B_x B_y}{\mu\mu_0} \; ; \; T_{xz} = \frac{B_x B_z}{\mu\mu_0} \; ; \\ T_{yx} &= \frac{B_y B_x}{\mu\mu_0} \; ; \; T_{yy} = \frac{B_y^2 - 0.5B^2}{\mu\mu_0} \; ; \; T_{yz} = \frac{B_y B_z}{\mu\mu_0} \; ; \\ T_{zx} &= \frac{B_z B_x}{\mu\mu_0} \; ; \; T_{zy} = \frac{B_z B_y}{\mu\mu_0} \; ; \; T_{zz} = \frac{B_z^2 - 0.5B^2}{\mu\mu_0} \; . \end{split}$$

Within the framework of the considered mathematical model, the dynamics of starting the serial UAD-32 IM (Fig. 1, a) were studied, the rotor of which was replaced by a solid one made of St3 steel (Fig. 3). The design and technical parameters of the electric motor are presented in Tabl. 1 and 2, respectively, its overall dimensions are shown in Fig. 1, b.

Table 1. Design data of UAD-32

Тип АД	D , MM	L, mm	$L_{ m l}$ , mm	l, mm	<i>a</i> , MM
UAD-32	50	70	108	19,5	4

Table 2. Nominal parameters of UAD-32

Rated electrical power $P_2$ , Watt	5		
Rotation speed <i>n</i> , rpm	2750		
Rated current $I_n$ , A	0,11		
Rated voltage, $U_n$ , V	220		
Number of phases	3		
Efficiency, %	25		
Multiplicity of maximum torque $M_m/M_n$	1,5		
Multiplicity of starting torque $M_s/M_n$	0,3		
Starting current multiplicity $I_s/I_n$	2,5		
Weight, kg	0,55		
Stator steel grade	E-31		
Rotor steel grade	E-31		
Steel sheet thickness, mm	0,35		
Rotor shaft steel grade	St45, carbon, structural		
Stator winding	two-layer, looped		
Operating mode	$S_1$		

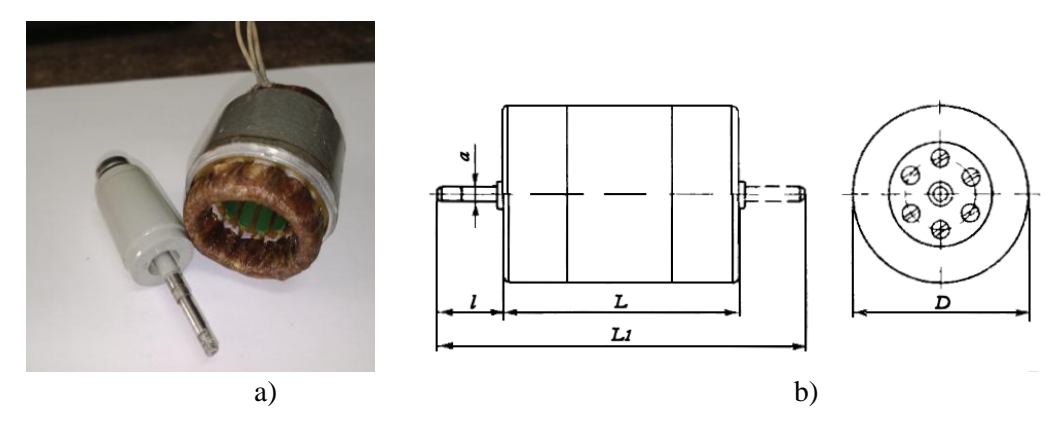


Fig. 1. Induction motor UAD-32 (a) and its dimensions (b)

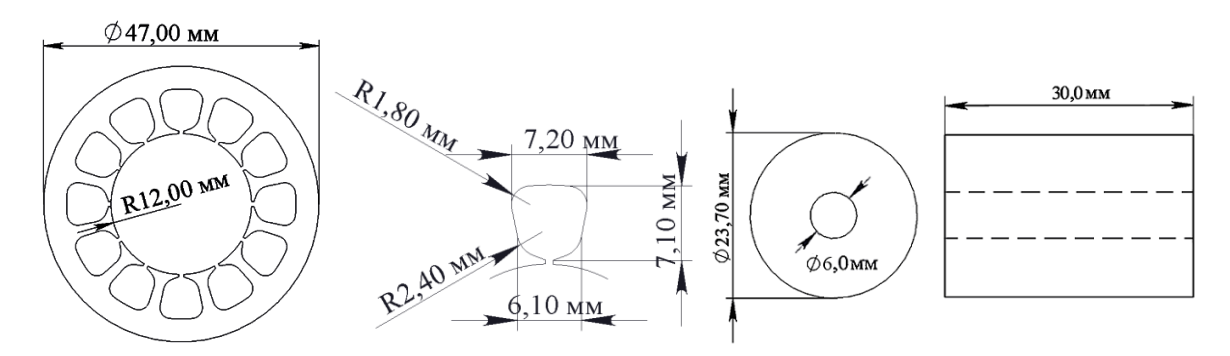


Fig. 2. Structural dimensions of the IMSR

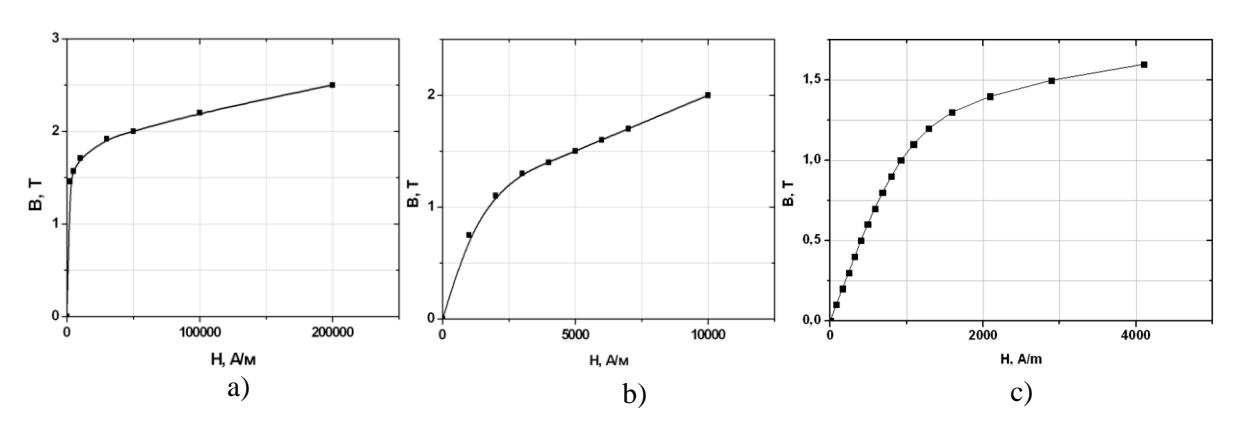


Fig. 3. Magnetization curves for steels: E-31 (a), St45 (b), St3 (c)

The stator package is assembled from sheets of electrical steel E-31 (Fig. 3, a) with a thickness of 0,35 mm, the rotor shaft is made of structural carbon steel St45 (Fig. 3, b), the active length of the package is 30 mm. Fig. 4, a shows an expanded diagram of a two-layer loop winding of an induction motor, Fig. 4, b — the distribution of winding phases by slots.

Based on the developed mathematical model of the IMSR, a simulation model was implemented that includes a finite element representation of an electric motor and an external electrical circuit together with a power source that forms a three-phase system of sinusoidal voltages with an amplitude of 311 V and a frequency of 50 Hz (Fig. 5).

The calculation of the combined model is performed for the mode of starting the IMSR without load with its subsequent loading up to  $M_{load}=0.1M_n$  at  $t_{load}=0.9\,$  s. As a result of the modeling, dynamic patterns of the distribution of the vector magnetic potential (Fig. 6) and magnetic induction (Fig. 7) in the cross-section of the IMSR for the moments of time  $t_1=0.1\,$ s and  $t_2=1.0\,$ s, respection

tively, are obtained. Based on the calculated data, graphs of transient processes of the angular velocity of the rotor (Fig. 8, a), the developed electromagnetic torque (Fig. 8, b), currents in the phases of the stator winding (Fig. 9) are constructed. The flux linkages of the stator winding phases and power losses in the solid rotor of the IMSR are shown in Fig. 10 and 11 respectively.

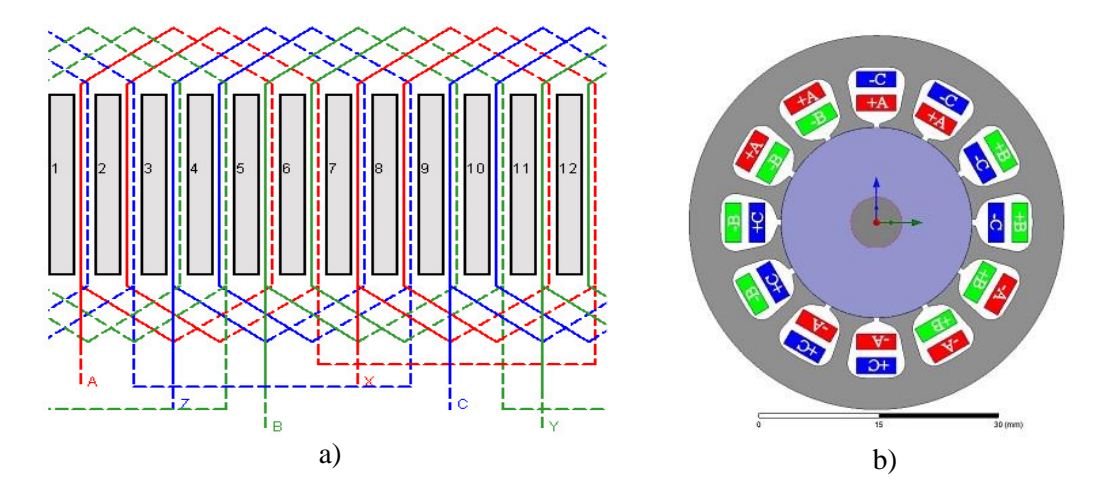


Fig. 4. Schematic diagram of the three-phase two-layer stator winding

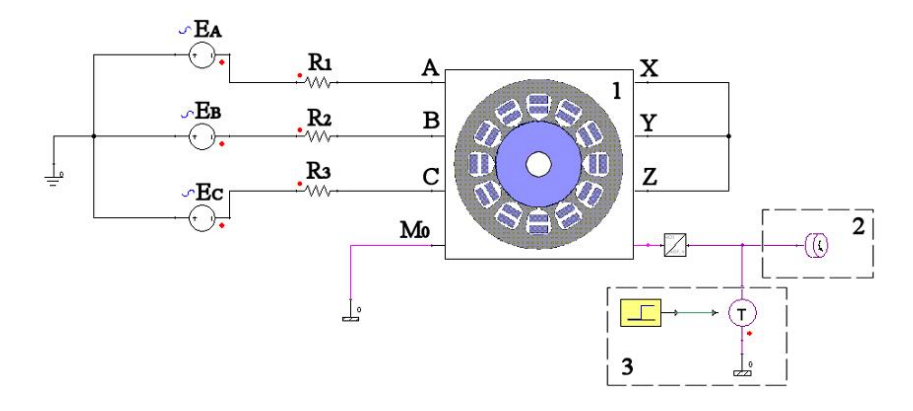


Fig. 5. Combined simulation model: 1 — finite element model of IMSR; 2 — rotor model; 3 — model for creating the moment of resistance on the shaft

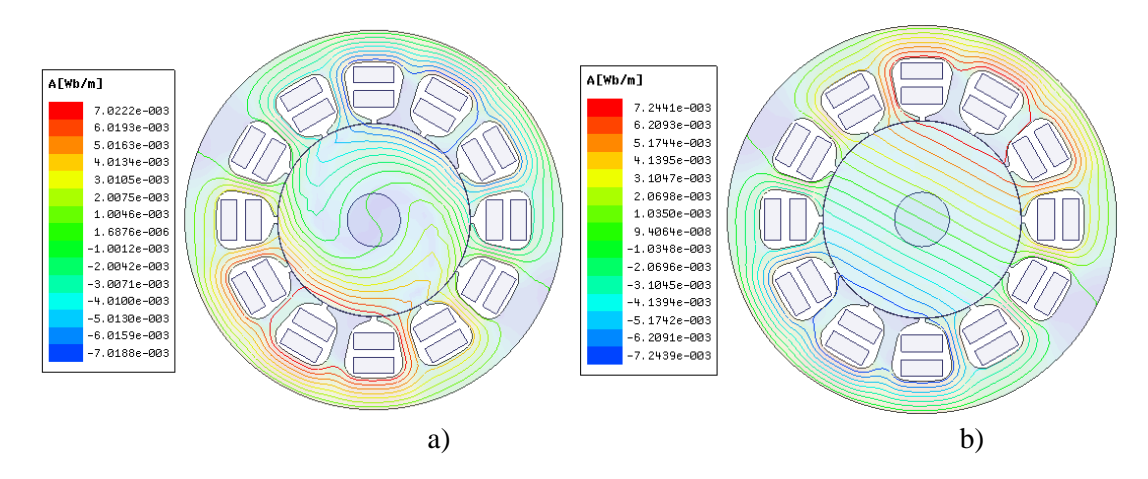


Fig. 6. Distribution of vector magnetic potential in the cross-section of the magnetic field with  $t_1 = 0.1 \, \text{s}$  (a) and  $t_2 = 1.0 \, \text{s}$  (b)

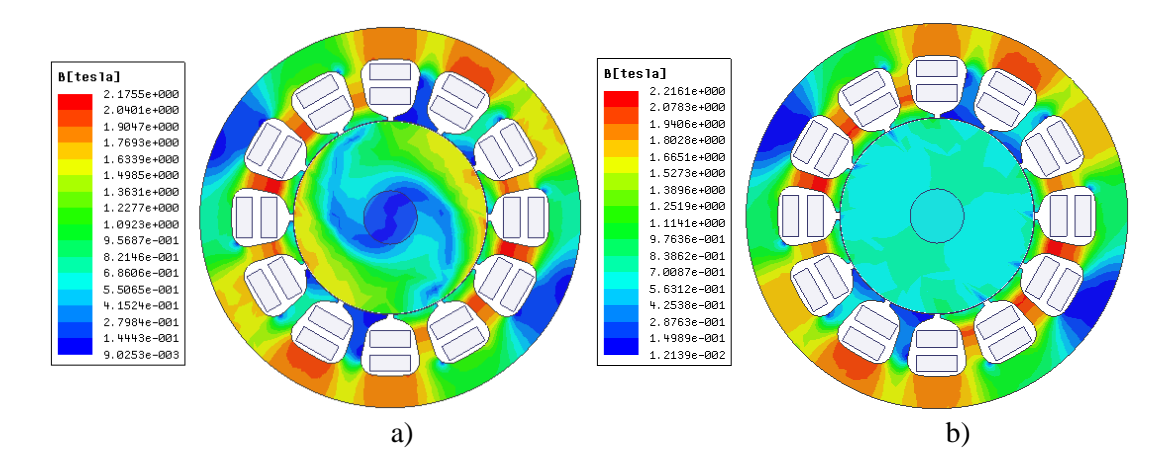


Fig. 7. Distribution of magnetic induction in the cross-section of the magnetic field with  $t_1 = 0.1$  s (a) and  $t_2 = 1.0$  s (b)

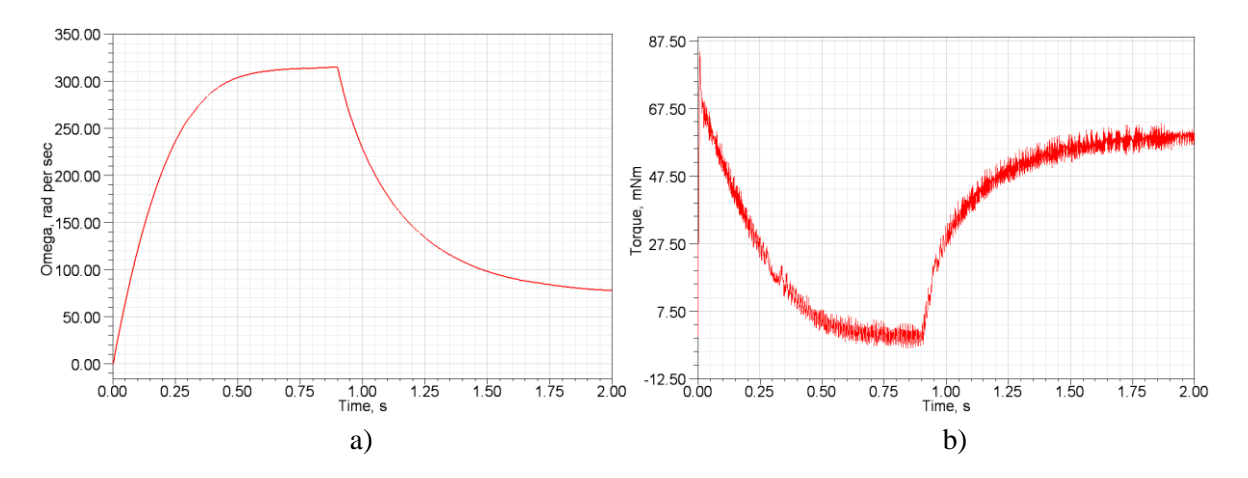


Fig.~8. Transient processes of the angular velocity of the solid rotor (a) and the electromagnetic torque of the IMSR (b)

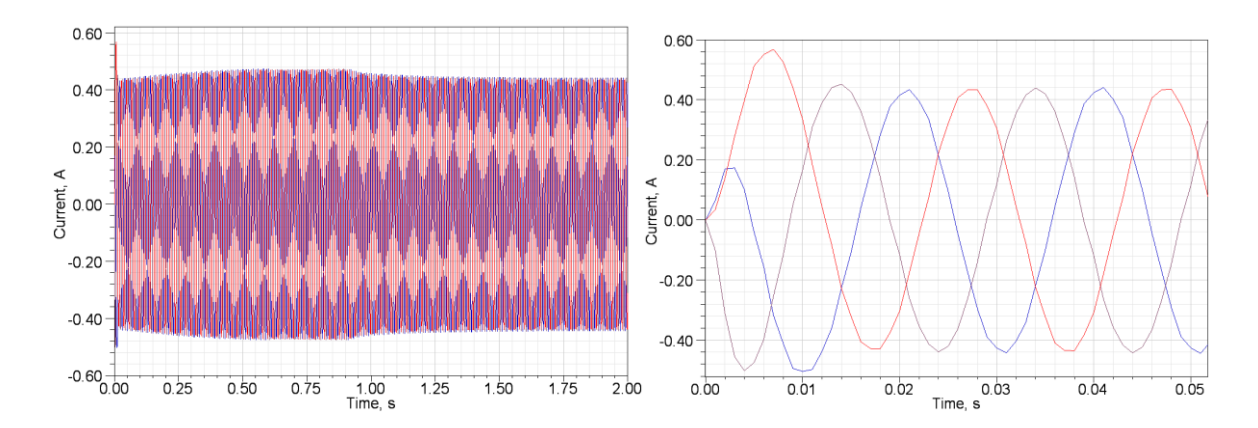


Fig. 9. Transient processes of currents in the rotor phases

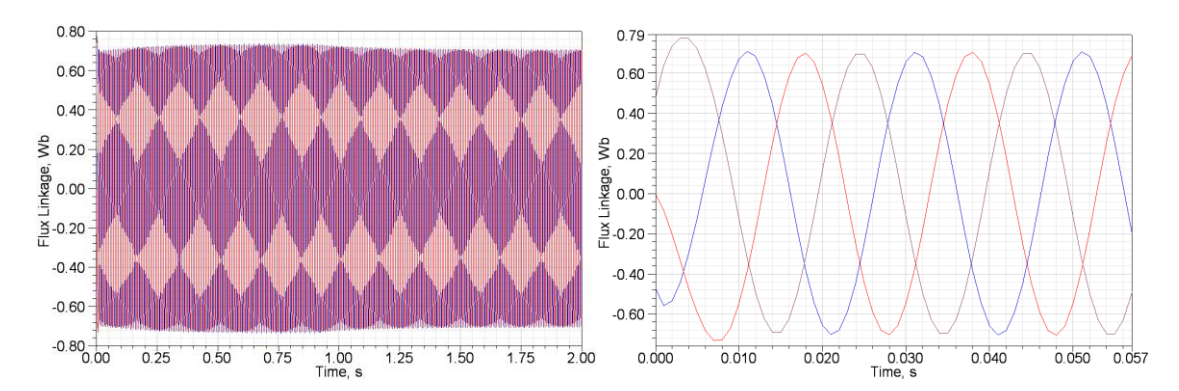


Fig. 10. Transient processes of stator winding flux linkages

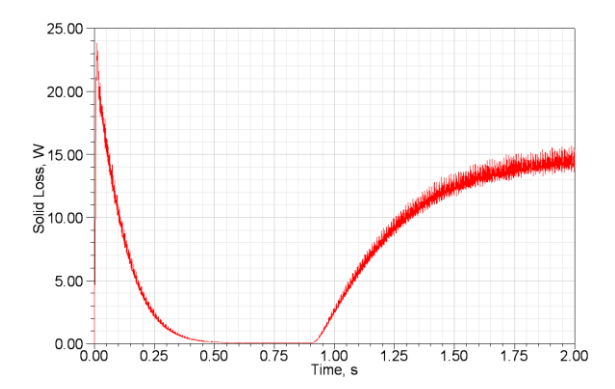


Fig. 11. Electric power losses in the solid rotor of the IMSR

#### **Conclusions**

Based on the results obtained, the following conclusions can be drawn: 1) a finite element model of an electric motor can be combined with an external electrical circuit containing a power source or a semiconductor converter, thereby forming a universal combined model for studying IMSR in dynamic modes; 2) it has been established that as the electric motor accelerates without load on the shaft ( $t = 0 \div 0.9$  sec), a vortex magnetic field behavior occurs in a solid rotor with the formation of local zones of increased magnetic flux density of about 1.9 T (Fig. 7, a). As the rotor reaches the ideal idling speed, the magnetic field is aligned inside its structure, while the slip value does not exceed several percent (Fig. 6, b); 3) the model calculation shows that the motor reaches the ideal idling speed in 0.9 seconds (Fig. 8, a), which exceeds the acceleration time serial UAD-32 ( $t_{ac\ time} = 0.3\ sec$ ). At the same time, the starting torque reaches the value of  $M_s = 80 \text{ mNm}$  (Fig. 8, b), and the starting current is  $I_s = 0.56 \,\mathrm{A}$  (Fig. 9). As the acceleration progresses, the current consumption does not decrease and stabilizes at I = 0,44 A, which is four times higher than the idle current of the serial motor  $(I = 0.11 \,\mathrm{A})$ ; 4) the electromagnetic torque does not have pronounced fluctuations, i.e. the acceleration of the motor occurs with a constant tractive effort on the shaft (Fig. 8, b). As the ideal idling speed is reached, the torque value decreases to the minimum values ( $M = 3 \div 4 \text{ mNm}$ ); 5) the application of the rated load ( $t = 0.9 \div 2.0$  sec) to the motor shaft leads to a significant decrease in the rotor rotation speed to the value of  $\omega = 80 \text{ rad/s}$  (more than 3,5 times) (Fig. 8, a), the electromagnetic moment increases to  $M = 52 \,\mathrm{mNm}$  (Fig. 8, b); 6) it has been found that in dynamic modes (acceleration, deceleration, overloading), significant power losses of tens of watts occur in the IMSR solid-state rotor (Fig. 11). Given the fact that an electric motor can be operated in repeated short-term modes, the amount of power released in these modes can have a critical effect on its temperature.

#### References

- 1. Bilek, V. & Barta, J. & Toman, M. & Losak, P. & Bramerdorfer, G. (2025). A comprehensive overview of high-speed solid-rotor induction machines: Applications, classification, and multiphysics modeling. International Journal of Electrical Power & Energy Systems, Vol. 166, 2025. https://doi.org/10.1016/j.ijepes.2025.110520.
- 2. D. Zhang, R. An, C. He, L. Bu, T. Wu. Electromagnetic design of a megawatt high efficiency high speed solid rotor induction motor. IEEE international electric machines and drives conference, IEMDC (2017), pp. 1-8, https://doi.org/10.1109/IEMDC.2017.8002095.
- 3. Arumugam, P. & Xu, Z. & Rocca, A.L. & Vakil, G. & Dickinson, M. & Amankwah, E. & Hamiti, T. & Bozhko, S. & Gerada, C. & Pickering, S.J. (2016). High-Speed Solid Rotor Permanent Magnet Machines: Concept and Design. IEEE Transactions on Transportation Electrification, Vol. 2, No. 3, 2016, p. 391-400.
- 4. Yi, J. & Zhu, Z. (2025). Design and analysis of electromagnetic and mechanical structure of ultrahigh-speed slotted solid rotor induction motor. Sci. Rep. 15, 2386 (2025). https://doi.org/10.1038/s41598-025-86405-0.
- 5. Zienkiewicz, O. & Taylor, R. & Govindjee, S. (2024). The Finite Element Method. Its Basis and Fundamentals (8th Edition). Butterworth-Heinemann.
- 6. Gadala, M. (2020). Finite Elements for Engineers with ANSYS Applications. Cambridge University Press.
- 7. Lee, H. (2023). Finite Element Simulations with ANSYS Workbench 2023. Theory, Applications, Case Studies. SDC Publications.
- 8. Logan, D. (2016). A First Course in the Finite Element Method. CL Engineering.
- 9. Pepper, D.W. & Heinrich, J.C. (2017). The Finite Element Method: Basic Concepts and Applications with MATLAB, MAPLE, and COMSOL (3rd Edition). CRC Press.
- 10. Aliprantis, D. & Wasynczuk, O. (2022). Electric Machines: Theory and Analysis Using the Finite Element Method. Cambridge University Press.
- 11. Li, G. (2020). Introduction to the Finite Element Method and Implementation with MATLAB. Cambridge University Press.
- 12. Cardoso, J.R. (2019). Electromagnetics through the Finite Element Method: A Simplified Approach Using Maxwell's Equations. CRC Press.
- 13. Kachura, A.V., & S'yanov, A.M., & Polyakov, R.M. (2017). Matematicheskoe modelirovanie zamknutoy sistemyi elektroprivoda na baze ventilnogo reaktivnogo dvigatelya na osnove metoda konechnyih elementov [Mathematical modeling of a closed loop electric drive system based on a reactive motor and finite elements method]. *Visnik natsionalnogo tehnichnogo universitetu «HPI» Bulletin of the National Technical University "HPI"*, 1, 1223, 113-117 [in Ukrainian].

## Список використаної літератури

- 1. V. Bilek, J. Barta, M. Toman, P. Losak, G. Bramerdorfer. A comprehensive overview of high-speed solid-rotor induction machines: Applications, classification, and multi-physics modeling. International Journal of Electrical Power & Energy Systems, Vol. 166. 2025. https://doi.org/10.1016/j.ijepes.2025.110520.
- 2. D. Zhang, R. An, C. He, L. Bu, T. Wu. Electromagnetic design of a megawatt high efficiency high speed solid rotor induction motor. IEEE international electric machines and drives conference, IEMDC (2017), pp. 1-8, https://doi.org/10.1109/IEMDC.2017.8002095.
- 3. P. Arumugam, Z. Xu, A.L. Rocca, G. Vakil, M. Dickinson, E. Amankwah, T. Hamiti, S. Bozhko, C. Gerada, S.J. Pickering. High-Speed Solid Rotor Permanent Magnet Machines: Concept and Design. IEEE Transactions on Transportation Electrification, Vol. 2, No. 3, 2016, p. 391-400.
- 4. J. Yi, Z. Zhu. Design and analysis of electromagnetic and mechanical structure of ultra-high-speed slotted solid rotor induction motor. Sci. Rep. 15, 2386, 2025. https://doi.org/10.1038/s41598-025-86405-0.
- 5. O. Zienkiewicz, R. Taylor, S. Govindjee. The Finite Element Method. Its Basis and Fundamen-

- tals. 8th Edition. Butterworth-Heinemann, 2024. 650 p.
- 6. M. Gadala. Finite Elements for Engineers with ANSYS Applications. Cambridge University Press, 2020. 626 p.
- 7. H-H Lee. Finite Element Simulations with ANSYS Workbench 2023. Theory, Applications, Case Studies. SDC Publications, 2023. 614 p.
- 8. D. Logan. A First Course in the Finite Element Method. CL Engineering, 2016. 992 p.
- 9. D.W. Pepper, J.C. Heinrich. The Finite Element Method: Basic Concepts and Applications with MATLAB, MAPLE, and COMSOL. 3rd Edition. CRC Press, 2017. 628 p.
- 10. D. Aliprantis, O. Wasynczuk. Electric Machines: Theory and Analysis Using the Finite Element Method. Cambridge University Press, 2022. 514 p.
- 11. G. Li. Introduction to the Finite Element Method and Implementation with MATLAB. Cambridge University Press, 2020. 522 p.
- 12. J.R. Cardoso. Electromagnetics through the Finite Element Method: A Simplified Approach Using Maxwell's Equations. CRC Press, 2019. 212 p.
- 13. Качура А.В., Съянов А.М., Поляков Р.М. Математическое моделирование замкнутой системы электропривода на базе вентильного реактивного двигателя на основе метода конечных элементов. Вісник національного технічного університету «ХПІ». Серія "Електричні машини та електромеханічне перетворення енергії". Х.: НТУ «ХПІ», 2017. № 1, 1223. С. 113-117.

Надійшла до редколегії 30.05.2025 Прийнята після рецензування 08.09.2025 Опублікована 23.10.2025